

# Novel nanosized AS1411–chitosan–BODIPY conjugate for molecular fluorescent imaging

This article was published in the following Dove Press journal:  
*International Journal of Nanomedicine*

Setareh Taki<sup>1</sup>  
Mehdi Shafiee Ardestani<sup>2</sup>

<sup>1</sup>Department of Radiopharmacy, International Campus, School of Pharmacy, Tehran University of Medical Sciences, Tehran, Iran; <sup>2</sup>Department of Radiopharmacy, Faculty of Pharmacy, Tehran University of Medical Sciences, Tehran, Iran

**Background:** In recent years, non-invasive imaging technologies for early cancer detection have drawn worldwide attention. In this study, an antinucleolin aptamer, AS1411, was successfully conjugated to BODIPY-labeled chitosan and studied on T47D and HEK-293 cell lines.

**Methods:** After conjugation of the aptamer to chitosan nanoparticles and purification, its structure was confirmed using atomicforce microscopy (AFM), electrophoretic light scattering (ELS) and dynamic light scattering (DLS). Results of AFM, DLS and ELS of both conjugation and chitosan were compared for confirmation of conjugation. Conjugates were mixed with BODIPY FL fluorescent dye, purified and lyophilized. The labeled conjugate was characterized using Fourier-transform infrared spectroscopy, ultraviolet–visible spectroscopy, ELS and DLS. In vitro cellular uptake and cytotoxic effects of BODIPY-labeled chitosan–AS1411 aptamer conjugates were evaluated using the XTT assay on T47D and HEK-293 cells and flow cytometry on T47D cells.

**Results:** The data showed that uptake of BODIPY-labeled chitosan–AS1411 aptamer conjugate was satisfactory. Moreover, there was no statistically significant cytotoxicity of the conjugate on either cell line.

**Conclusion:** The outcomes confirmed the potential application of this new targeted imaging agent as a novel cancer diagnostic agent for molecular imaging.

**Keywords:** AS1411, chitosan, BODIPY, molecular imaging

## Introduction

Based on recent cancer incidence data,<sup>1</sup> it was anticipated that in the USA, about 2 million new cases and 600,000 deaths from cancer would occur in 2018. In 2014, the WHO reported that breast cancer had the highest number of cases and deaths among Iranian women.<sup>2–4</sup>

Since drug-resistant breast cancer is one of the most important health problems nowadays, detection of disease in the early stages can help physicians to use the right drug by determining which type of cancer is growing in the patient's body. Earlier diagnosis and intervention may help to reduce costs and the course of treatment. Although scientists have used a number of methods for cancer diagnosis, including endoscopy,<sup>5</sup> physical examination,<sup>6</sup> biopsy,<sup>7</sup> genetic tests<sup>8</sup> and imaging,<sup>9</sup> targeted imaging techniques can be more powerful in determining the precise location, size and metastasis of the tumor. Moreover, finding the right targeting agent depends on a full understanding of the overexpressed receptors on the surface of the individual's cancer cells and/or using a proper and widespread biomarker on the cancer cell surface. Nucleolin is a biomarker (protein) which exists specifically

Correspondence: Mehdi Shafiee Ardestani  
Department of Radiopharmacy, Faculty of Pharmacy, Tehran University of Medical Sciences, 3183815194, Tehran, Iran  
Tel +98 21 2204 8173  
Email Shafieeardestani@tums.ac.ir

on the cancer cell membrane.<sup>10</sup> As nucleolin is not over-expressed on the normal cell surface, it can be used as a good biomarker for determining the cancer cells using an appropriate targeting agent (eg, aptamer, antibody or peptide). AS1411 aptamer is an anticancer drug which has entered the second phase of clinical trials for the treatment of metastatic renal cell carcinoma. This aptamer can target various types of cancer cells via nucleolin shape complementarity.<sup>11–15</sup>

In biomedical nanotechnology, nano-structures are used for delivering drugs and imaging agents to the location of interest. This method helps to reduce the off-target delivery of the drug/agent and consequently decreases the toxicity of the drug or increases the precision of imaging.<sup>16</sup> Many different nano-structures are used in drug/contrast agent delivery, such as liposomes, albumin-bound and polymeric structures, quantum dots, gold and iron oxides.<sup>17–19</sup>

Chitosan is an exciting cationic polymer which has been exploited broadly in different fields of the medical sciences. Chitosan is a biocompatible, biodegradable, anti-bacterial, antifungal and non-toxic natural polymer which can be used as a potential drug carrier. Moreover, researchers use chitosan to coat other forms of nano-structure which are made of other materials, to elevate their bio-availability and reduce their unwanted effects on the body.<sup>16,20,21</sup> Cationic nanoparticles can overcome the off-target limitation of drugs/agents when they are applied in the human body. On the other hand, positively charged nanoparticles are more cytotoxic than negatively charged nanoparticles because they have disruptive interactions with cell membrane components during their uptake into the cells. Moreover, they show more instability, fast clearance and aggregation.<sup>22,23</sup> Previously, Behrouz et al<sup>28</sup> constructed a novel anticancer agent using 5-fluorouracil (5-FU)-conjugated PAMAM–AS1411 aptamer conjugates for cancer therapy. Although this study showed promising effects in cancer therapy, PAMAM itself was toxic to normal cells owing to its positive nature. Therefore, our project focused on using chitosan along with a negatively charged aptamer (AS1411) to balance the nano-structure surface charge and overcome the above-mentioned limitations.

Optical imaging is a technique for non-invasively looking inside the body. It uses visible light and the special properties of photons to obtain detailed images of organs and tissues, as well as smaller structures including cells and even molecules. Although in vivo

nano-optical imaging has not yet been used clinically, it is attracting attention as a new research tool for the following reasons. First, it significantly reduces patient exposure to harmful radiation by using non-ionizing radiation. The types of light used generate images by exciting electrons without causing the damage that can occur with the ionizing radiation used in some other imaging techniques. Because it is much safer for patients, and significantly faster, optical imaging can be used for lengthy and repeated procedures over time to monitor the progression of disease or the results of treatment. Second, it is particularly useful for visualizing soft tissues. Soft tissues can be easily distinguished from one another because of the wide variety of ways different tissues absorb and scatter light. Third, various colors of light provide an advantage by enabling many different properties of an organ or tissue to be seen and measured at the same time. Other imaging techniques are limited to just one or two measurements.<sup>24,25</sup> This research, for the first time, aimed to prepare a novel optical diagnostic agent for breast cancer imaging using BODIPY-labeled AS1411 aptamer–chitosan conjugates. The novel diagnostic agent was tested for its toxicity, safety and cellular uptake.

## Materials and method

### Materials

AS1411 aptamer was purchased from TAG (Copenhagen, Denmark). N,N'-Dicyclohexylcarbodiimide (DCC), chitosan nanoparticles and CaCl<sub>2</sub> were supplied by Merck (Darmstadt, Germany). N-Hydroxysuccinimide (NHS) and 1-ethyl-3-(3-dimethylaminopropyl) carbodiimide hydrochloride (EDC) were obtained from Sigma-Aldrich (St Louis, MO, USA). HEK-293 and T47D cell lines were purchased from the Pasteur Institute of Iran (Tehran, Iran). Dynamic light scattering (DLS) and electrophoretic light scattering (ELS) to measure the zeta potential were performed using a Malvern Nano ZS (Malvern Instruments, Malvern, UK). Atomic force microscopy (AFM) images were captured using a NanoWizard II (JPK Instruments, Berlin, Germany). Fourier-transform infrared spectroscopy (FT-IR) experiments were conducted using a Perkin Elmer Spectrum BX-II spectrometer (Nizhni Novgorod, Russia). All other chemical reagents were of analytical grade and used without additional purification. The animal experiments were approved by the Tehran University of Medical Sciences (number IR.TUMS.PSRC.REC.1396.2340) and followed the guidelines of the university ethics committee.

## Aptamer shape preparation

The 26 bp AS1411 aptamer with the sequence 5'-carboxy-C10-GGTGGTGGTGGTTGTGGTGGTGGTGG-3' was purchased from TAG (Copenhagen, Denmark). The aptamers needed to form their proper shape using heating and cooling sections. For this purpose, lyophilized aptamers were dissolved in 0.5 mL deionized water, then heated to 85°C for 2 minutes and then cooled in the laboratory to reach room temperature (25°C) for 10 minutes. This strategy helps aptamers to shape appropriately and fixes their proper form for shape-complementary targeting purposes.

## Chitosan-aptamer conjugation

Chitosan nanoparticles (Merck, Darmstadt, Germany) were conjugated with carboxylated AS1411 aptamer using their amine groups, as follows. To the vial containing the aptamer, 5 mL dimethyl sulfoxide (DMSO) (Merck, Darmstadt, Germany), 100 mg EDC and 0.0071 mg NHS (Sigma-Aldrich, St Louis, MO, USA) and sufficient CaCl<sub>2</sub> (Merck, Darmstadt, Germany) were added. The composition then mixed with 100 mg of the chitosan and stirred for 24 hours under ambient conditions. Thereafter, samples were purified using a centrifuge (40,000 rpm for minutes), lyophilized and stored at -20°C for further use.

## BODIPY FL-labeled conjugates

Conjugates were mixed with BODIPY FL-carboxylic acid dye (1:2 molar ratio) in the presence of EDC and NHS. The mixture was stirred for 20 minutes at 25°C. Subsequently, the labeled conjugates were purified using a dialysis bag against double-distilled water (1 L) for 24 hours and lyophilized. Labeled conjugates were characterized by fluorescence spectrometry at 460 nm, FT-IR, DLS and ELS compared to chitosan and other controls.

## AFM imaging

AFM images of the AS1411-chitosan conjugates and plain chitosan were recorded in double-distilled water using a NanoWizard II at 25°C on a microscope slide, using intermittent contact mode (air) for conjugates and contact mode for chitosan. Differences between the images show the conjugation.

## Hydrodynamic size distribution (DLS) and zeta potential (ELS)

DLS and ELS of AS1411-chitosan conjugates and plain chitosan were measured at a wavelength of 633 nm with

an OD of 0.3 using a He-Ne laser at room temperature. Results were then compared to each other.

## FT-IR

Using a Perkin Elmer Spectrum BX-II spectrometer, the infrared spectrum was evaluated to confirm the synthesis of the labeled AS1411-chitosan conjugates.

## Molar mass measurement of the conjugate using static light scattering

The static light scattering procedure followed the previous method<sup>26</sup> at five different concentrations of the conjugate (1, 0.8, 0.6, 0.4 and 0.2 mg/mL) in deionized, pre-filtered water at room temperature. Perfect synthesis of the conjugation process was confirmed by comparison between the molecular weights of the conjugate and chitosan.

## Fluorescence spectroscopy

Fluorescence spectroscopy was conducted at 460 nm to confirm the labeling process.

## Anti-proliferative evaluation using XTT assay

For the XTT assay, cells were cultured in RPMI and DMEM (supplemented with 10% FBS in a 5% CO<sub>2</sub> humidified incubator). The cytotoxicity of BODIPY FL-labeled AS1411-chitosan conjugates was measured after 24 and 48 hours for T47D and after 48 hours for HEK-293 cells at 50, 100, 150, 200 and 400 mg/mL concentrations, at 450 nm, using ELISA plate readers (BioTek Instruments, Northern Vermont, USA). Data were analyzed using Prism 5 statistical software (n=3, P<0.05 statistically significant) via one-way ANOVA followed by the Tukey test.

## Histopathological study

The animals were killed at 2 days post-injection and the harvested tissues (liver, kidney, heart and spleen) were fixed in 10% neutral-buffered formalin (pH 7.26) for 48 hours, then embedded in paraffin. The 5-µm-thick sections were prepared and stained with H&E. The histological slides were evaluated by an independent reviewer, using light microscopy (Olympus BX51; Olympus, Tokyo, Japan). Any changes, including acute and chronic inflammatory responses, fatty changes, coagulative necrosis, hemorrhage and hyperemia, were considered.

## In vitro cellular uptake using flow cytometry

To measure cellular uptake,  $2 \times 10^6$  T47D cells were seeded in six-well plates. After 24 hours,  $10^6$  cells were treated with BODIPY FL-labeled AS1411–chitosan conjugates (concentration 50 mg/mL) and the rest remained untreated as a control. Cells were incubated for 6 hours. The cells were trypsinized and collected after incubation. Then, they were centrifuged and washed with PBS. Afterwards, cells were resuspended. Then,  $10^4$  cells per sample were taken to carry out flow cytometry.

## In vivo fluorescence imaging

For fluorescence in vivo imaging, all mice were anesthetized with ketamine 100  $\mu$ g/mL. BODIPY FL-labeled conjugates were injected into mice ( $n=3$ ) through the tail vein. Images were acquired 1 and 2 hours after injection.

## Results

### Characterization of BODIPY FL-labeled chitosan–aptamer conjugates

Figure 1 displays the chemical synthesis of the labeled nano-conjugate. An FT-IR spectrum of the conjugate is shown in Figure 2. FT-IR spectrum wave numbers of chitosan are: 3416.32 (OH), 2873.62 (CH stretching), 1638.97 (CO carbonyl), 1520.07 (NH), 1423.83 (CH-OH) and 1384.20 ( $\text{CH}_2\text{-OH}$ )  $\text{cm}^{-1}$ . FT-IR spectrum wave numbers of the conjugates labeled with BODIPY FL are: 953.46 (PO bond in the phosphates), 3431.23 (OH), 3005.42 (CH stretching), 1661.31 (CO carbonyl), 1407.24 (C=N) and 1316.81 (C=C)  $\text{cm}^{-1}$ . DLS and ELS graphs of labeled AS1411–chitosan conjugates, AS1411–chitosan conjugates and plain chitosan are shown in Figure 3. Based on the results, size=60 nm and zeta potential=13.4 mV were obtained for the chitosan, and size=106 nm and zeta potential=-5.25 mV were obtained for the conjugates. As is obvious from the results, the size of the particles

5'-carboxy-C10-GGT-GGT-GGT-GGT-TGT-GGT-GGT-GG-3'

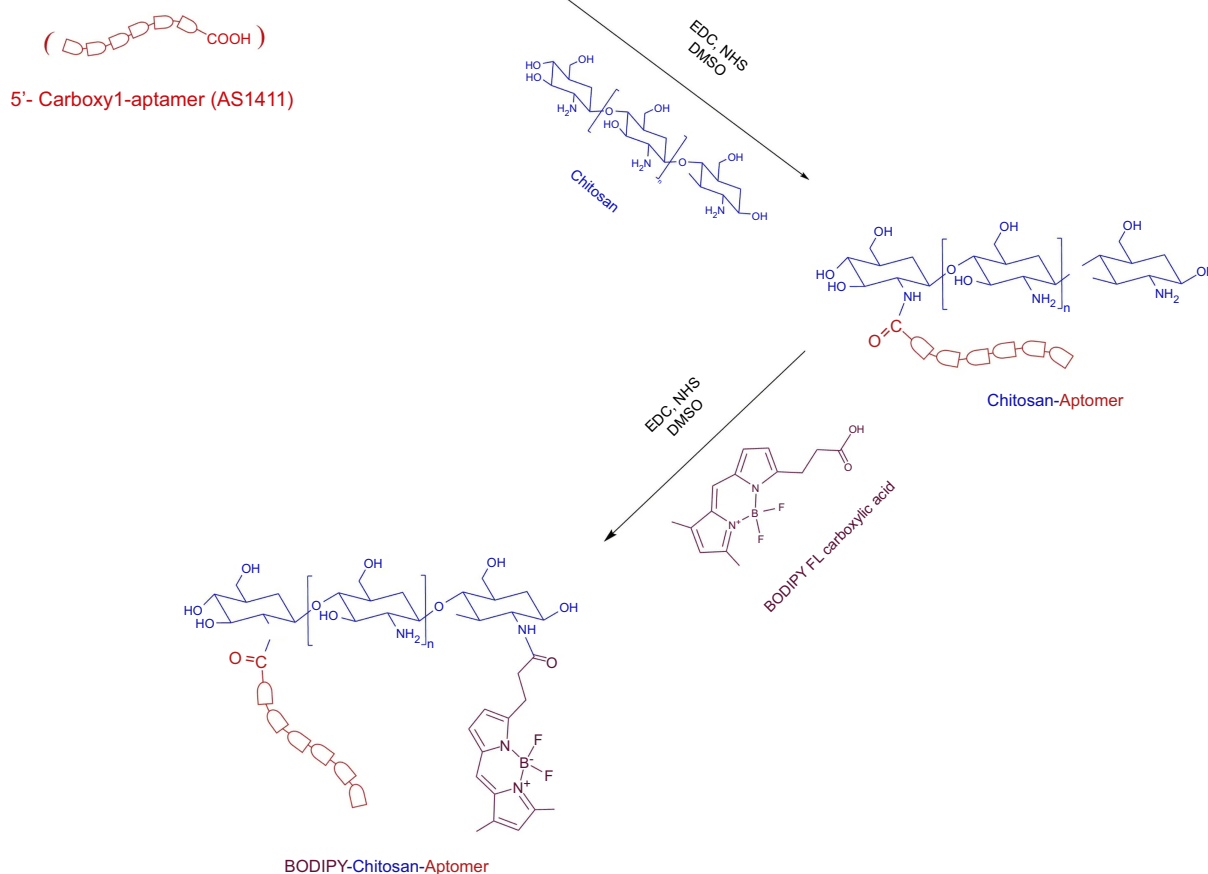
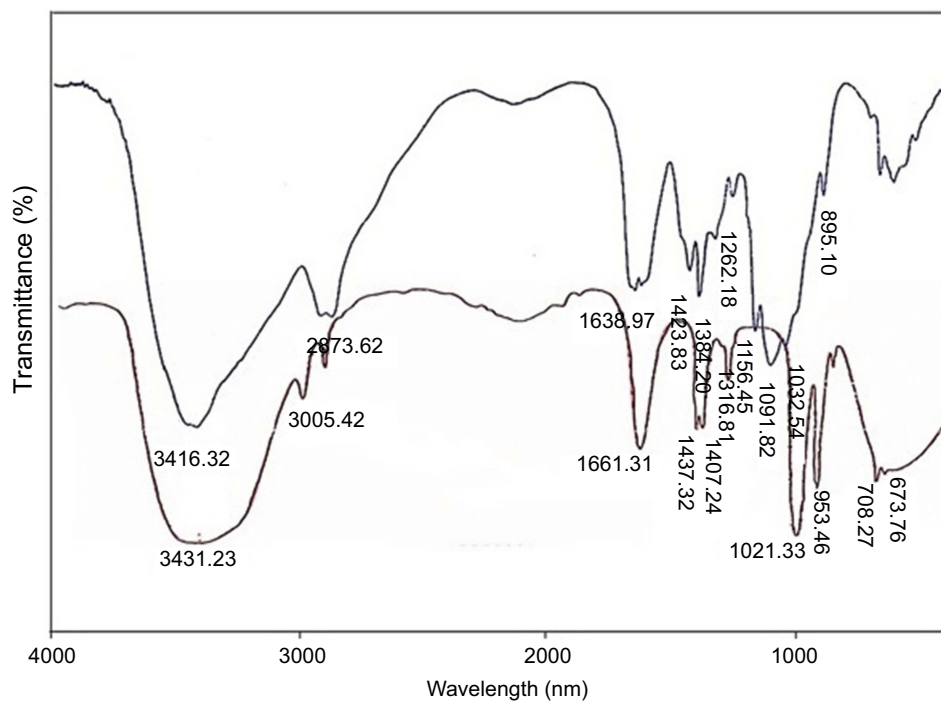
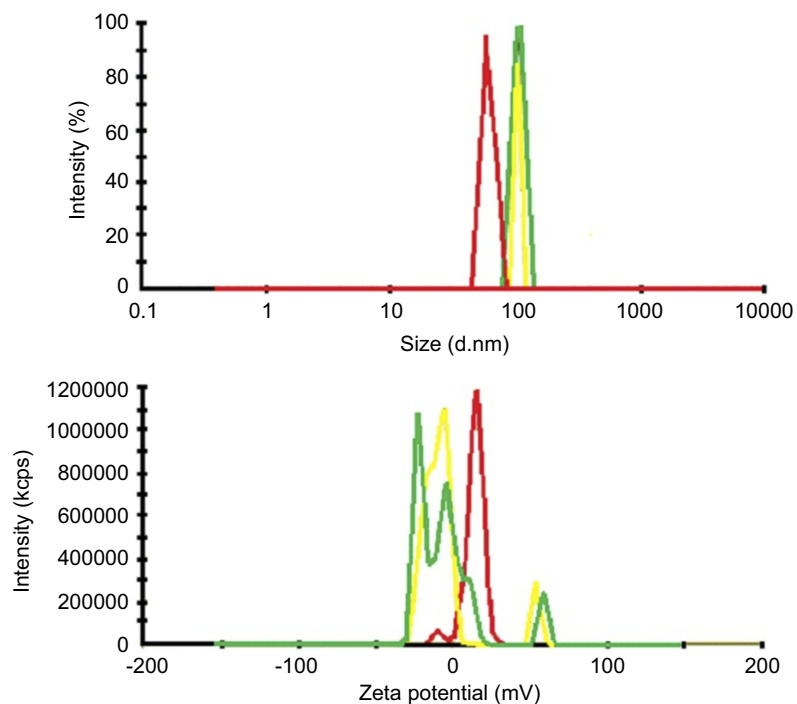


Figure 1 Synthesis of the labeled nano-conjugate.



**Figure 2** Fourier-transforminfrared spectroscopy images of chitosan (blue) and conjugates labeled with BODIPY FL (red).



**Figure 3** Size and zeta potential of chitosan (red), chitosan-aptamer conjugates (yellow) and labeled chitosan-aptamer conjugates (green).

increased and their zeta potential became more negative after conjugation with a negatively charged aptamer. These results confirm the correct synthesis of the chitosan and conjugate. The increased size of the conjugate shows the perfect conjugation. Also, the reduced

zeta potential of the labeled conjugate confirms that labeling was done successfully. AFM images of the AS1411-chitosan conjugates and plain chitosan are shown in Figure 4. It can be seen in these images that the conjugates are more spherical in their two-

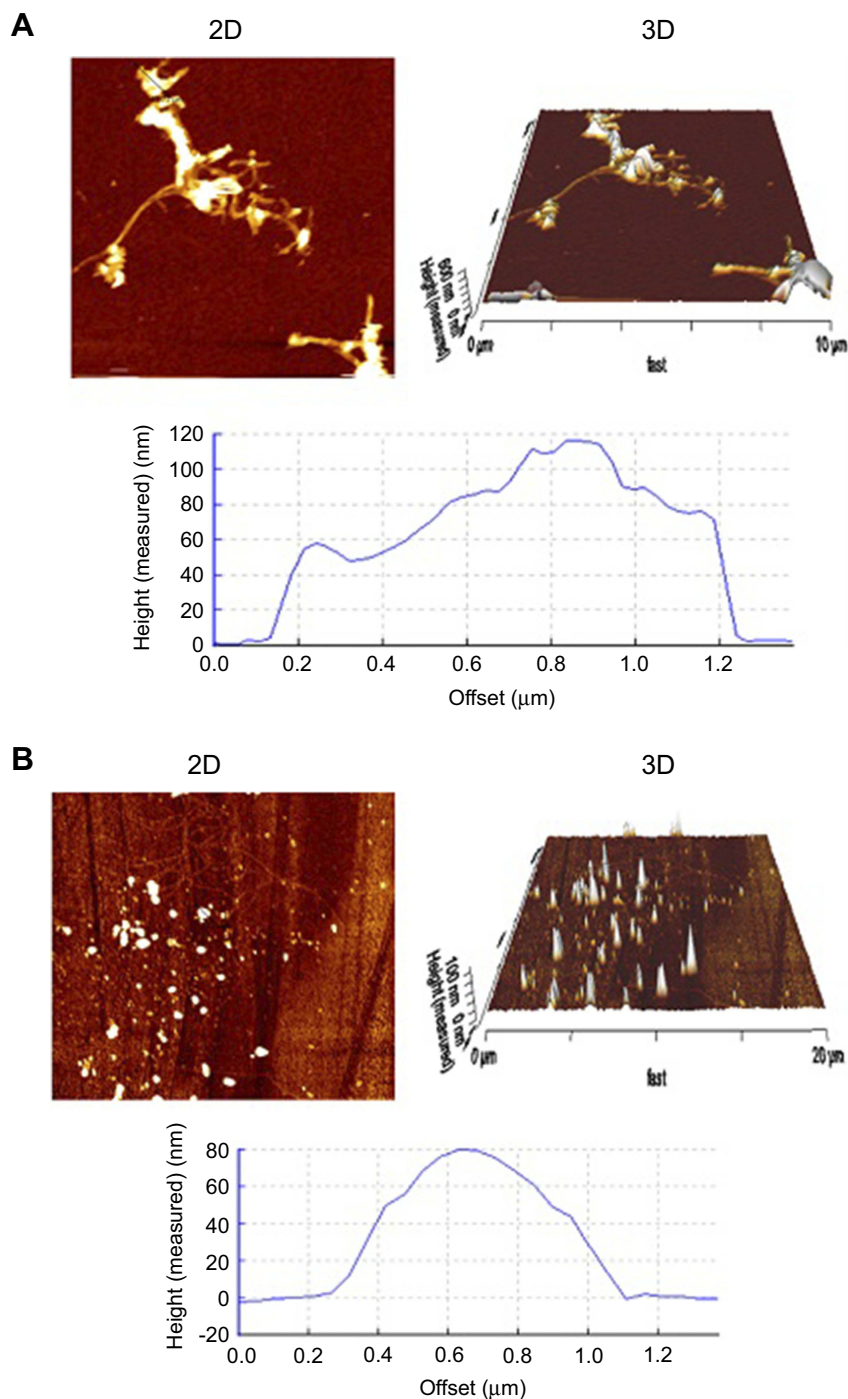


**Figure 4** Atomic force microscopy images of **(A)** chitosan and **(B)** aptamer–chitosan conjugates. Conjugates are more spherical in their two-dimensional (2D) shape and conical in the three-dimensional (3D) image in comparison to the plain chitosan.

dimensional shape and conical in the three-dimensional image in comparison to the plain chitosan. The cross-sectional graphs measure the physical values of the particles. From the cross-sectional graphs, the characteristics of the particles were measured, including the physical size (both  $10.00 \times 10.00 \mu\text{m}$ ), average

roughness  $R_a$  (chitosan  $32.08 \text{ nm}$ ; conjugate  $28.62 \text{ nm}$ ), root mean square roughness  $R_q$  (chitosan  $37.96 \text{ nm}$ ; conjugate  $31.00 \text{ nm}$ ) and peak-to-valley roughness  $R_t$  (chitosan  $115.5$ ; conjugate  $82.33 \text{ nm}$ ). The average molecular weight for the conjugate was  $7.06 \pm 0.624 \text{ kDa}$ , as shown in Figure 5. Results obtained from

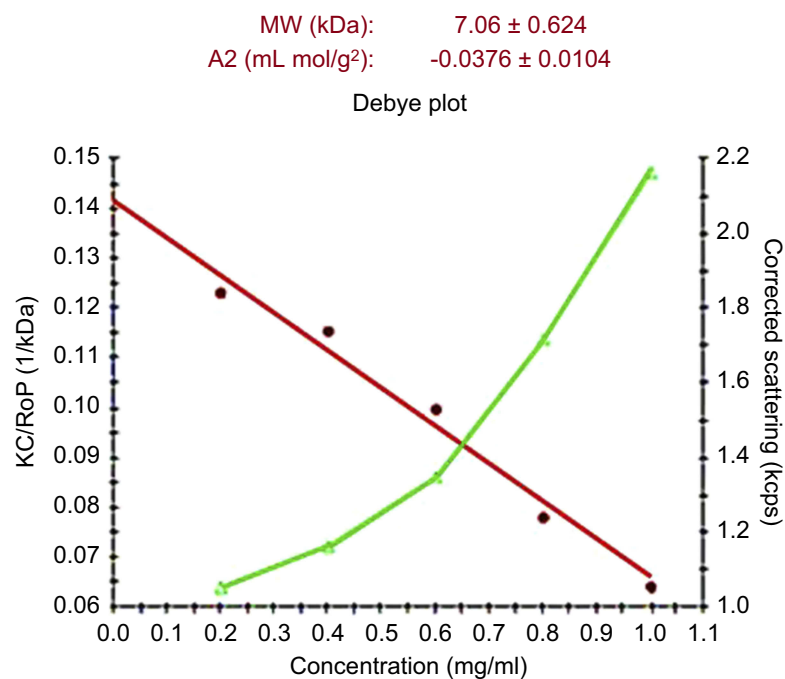


**Figure 5** Debye plot of the conjugate.

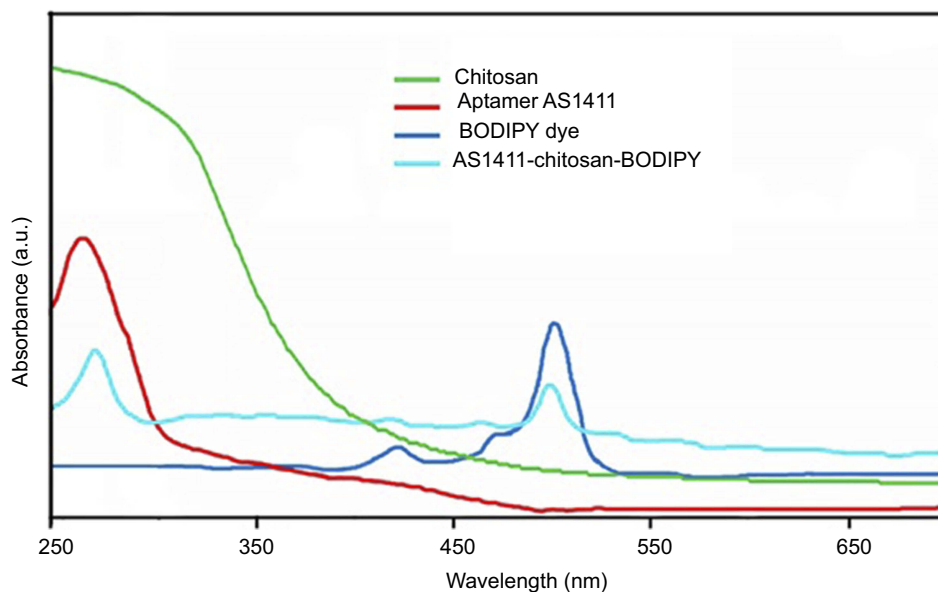


**Figure 6** Ultraviolet-visible spectroscopy of chitosan, aptamer AS1411, BODIPY dye and AS1411-chitosan-BODIPY conjugate.

ultraviolet-visible (UV-Vis) spectroscopy (Figure 6) and fluorescence spectroscopy (Figure 7) confirmed that the labeling process was done perfectly.

### Anti-proliferative evaluation using XTT assay

Based on the statistical analysis of data yielded by the XTT assay, BODIPY FL-labeled AS1411-chitosan

conjugates had no significant toxicity on any of the T47D cells at 24 hours after treatment or HEK-293 cells at any concentration. On the other hand, for T47D cells at 48 hours after treatment, it showed significant toxicity at all concentrations. Data were analyzed using Prism 5 statistical software ( $n=3$ , mean  $\pm$  SEM,  $P<0.05$  statistically significant) via one-way

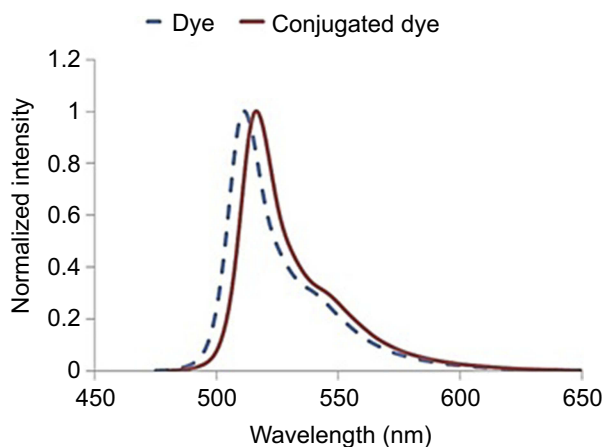


**Figure 7** Fluorescence spectroscopy of labeled conjugate.

ANOVA followed by the Tukey test. Graphs are presented in Figure 8.

## Histopathological study

All H&E-stained tissue sections from control and treatment groups were evaluated histologically. Micrographs of control tissues showing the normal cells are presented in Figures 9 and 10. Micrographs of treated tissues showed no histopathological changes in liver and hepatic cords. There was no sign of sinusoidal congestion. In general, data obtained from the histopathological study showed no indication of inflammatory response or necrosis in cells indicating *in vivo* toxicity in tumor tissues, as shown in Figure 11.

## In vivo fluorescence imaging

To evaluate the uptake of conjugates, fluorescence imaging was acquired at two different times. Figure 12 shows the accumulation of AS1411–chitosan labeled with BODIPY FL 1 and 2 hours post-injection in the tumor site compared to the control group. Accumulation in the liver (Figure 13) was clearly visualized at 2 hours after injection, indicating that metabolism of labeled AS1411–chitosan was probably taking place in the liver.

## In vitro cellular uptake using flow cytometry

Flow cytometry data (Figure 14) show an appropriate uptake (58%) of labeled conjugate into the T47D cells (red). The black graph is the untreated T47D control.

## Discussion

In this study, for the first time, AS1411 aptamer was conjugated to the chitosan nano-structure and the conjugates were labeled with BODIPY FL for cancer diagnosis applications. For this purpose, chitosan nanoparticles were conjugated with the aptamer using DMSO, EDC and NHS. To label the conjugate with BODIPY FL, they were mixed together. Formation of conjugation was confirmed using DLS, ELS, FT-IR, UV-Vis and AFM. Based on the peaks obtained from the areas of  $1638\text{ cm}^{-1}$  in the chitosan and  $1653\text{ cm}^{-1}$  in the conjugates, which, respectively, represent amines in the chitosan and amide bonds between the chitosan and aptamers in the conjugate, it can be concluded that proper conjugation has taken place. The increase in the conjugate size compared to intact chitosan demonstrated that conjugation was done perfectly. The reduced zeta potential of the labeled conjugate confirmed that labeling was successful. Data yielded from AFM spectroscopy confirmed the size of the nano-structure. UV-Vis spectroscopy showed clear and sharp peaks around 260 and 500 nm, indicating the conjugation of aptamer AS1411 and BODIPY dye, respectively. The shift in the maximum intensity of the labeled conjugate to longer wavelengths, validated by fluorescence spectroscopy, indicated that the labeling process was successful and suitable uptake of labeled conjugate in T47D cells had taken place.

Mohammadzadeh et al<sup>27</sup> constructed a novel cancer diagnostic agent using AS1411 aptamer–anionic linear globular dendrimer–G<sub>2</sub> conjugates carrying a contrast agent (Iohexol). They used different *in vitro* and *in vivo* tests to evaluate the imaging ability, safety and targeting nature of the drug. They also reported that this new diagnostic agent has no toxicity in normal tissues, so it can specifically target cancer cells. The targeted nature of the diagnostic agent makes it a promising tool for tumor computed tomography (CT) imaging.

Previously, Behrouz et al<sup>28</sup> used the same aptamer (AS1411) conjugated with PAMAM dendrimer–PEG carrying 5-FU for the treatment of gastric cancer. They labeled the dendrimer with BODIPY FL. Their targeted nanomedicine showed promising results in reducing the number of cancer cells, as well as non-toxicity of the drug *in vitro* and *in vivo*.

Positively charged nanoparticles such as PAMAM have a major drawback, which is related to their charge. Positively charged nanoparticles are more toxic than neutral or negatively charged nanoparticles because they form

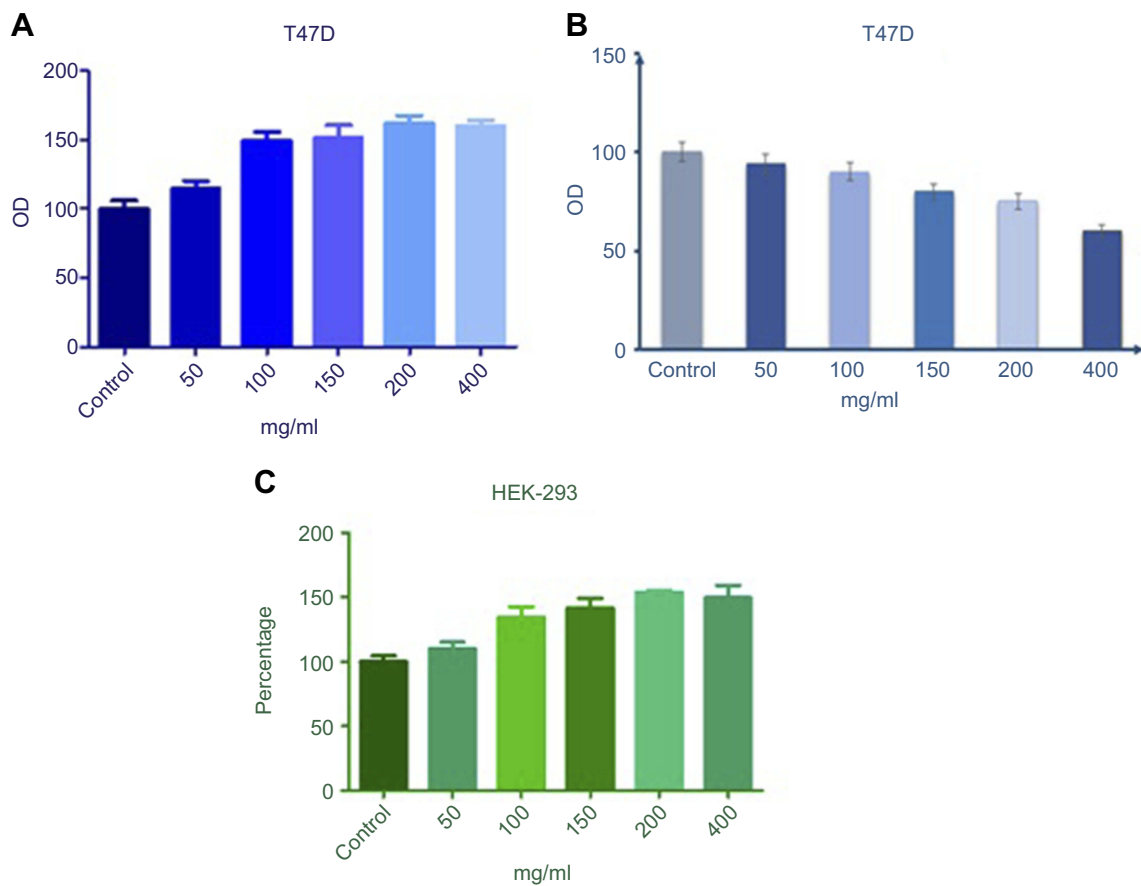


**Figure 8** XTT assay results of BODIPY FL-labeled ASI411-chitosan conjugates on T47D cells at **(A)** 24 hours and **(B)** 48 hours, and **(C)** on HEK-293 cells (n=3, data presented as mean  $\pm$  SEM).

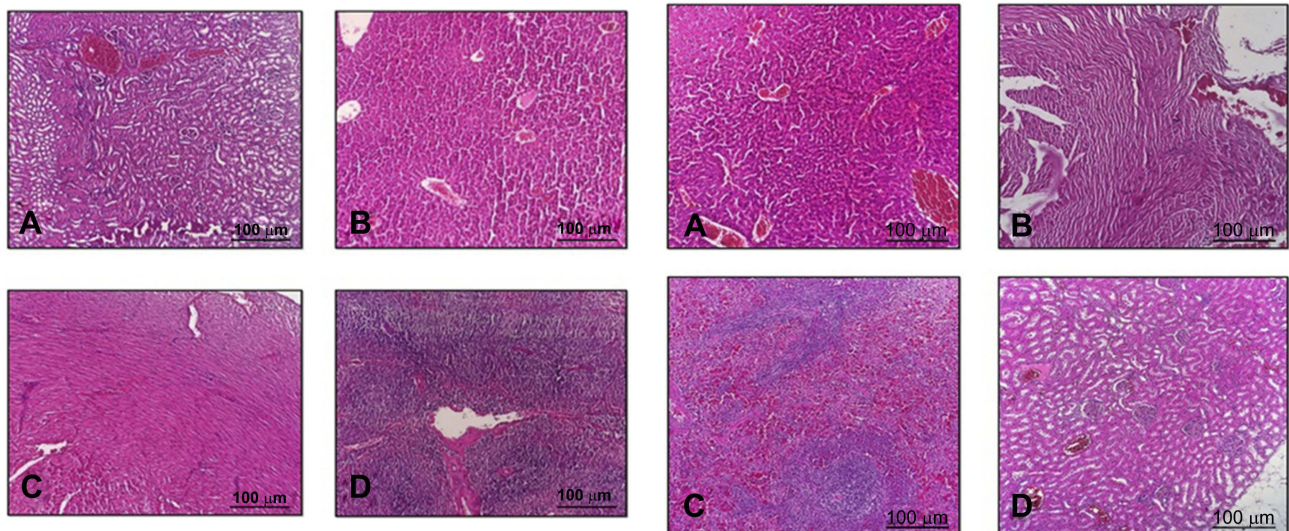


**Figure 9** Histopathological sections of **(A)** kidney, **(B)** liver, **(C)** heart and **(D)** spleen in the control group. H&E stain,  $\times 100$ .

**Figure 10** Histopathological sections of **(A)** liver, **(B)** heart, **(C)** spleen and **(D)** kidney in the treatment group. H&E stain,  $\times 100$ .

unwanted interactions with the negatively charged cell membrane.<sup>23</sup> Thus, in this study, a positively charged chitosan was used with a negatively charged aptamer to

form a negatively charged conjugate, which ensures the safety of this newly prepared conjugate for normal cells in the body.

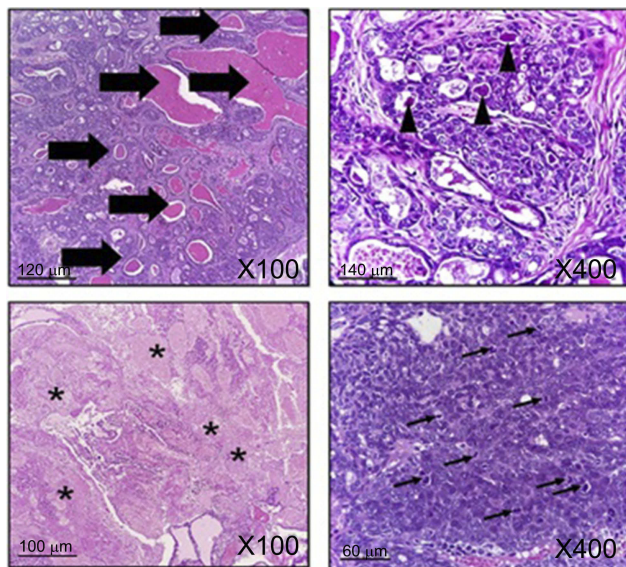


**Figure 11** Histopathology of treated breast cancer. Thick arrows: glandular formation; arrowheads: bizarre cell formation; asterisks: massive necrosis; thin arrows: mitotic figures. H&E stain.

As clearly shown in the anti-proliferative assay, the prepared conjugate had no toxicity on normal cells (HEK-293) at any concentration. Also, there was a slight increase in the number of cells after treatment with increasing concentrations

of the conjugate. The conjugate showed cytotoxicity on T47D cells 48 hours after treatment. These results confirmed the data obtained from the histopathological assay. Therefore, it can be used as a safe diagnostic and therapeutic agent for cancer detection and treatment. According to findings from the histopathological assay, tissues were normal and the toxicity did not occur in normal tissue, but increased cell death was observed in tumor tissue compared with the control group.

A number of aptamers are used as anticancer drugs, such as MUC-1,<sup>29</sup> AS1411<sup>30</sup> and A10 aptamers.<sup>31–34</sup> Sayari et al designed a novel targeted carrier for a poorly soluble, highly toxic anticancer drug (SN38). They used MUC-1 aptamer conjugated with chitosan nanoparticles as a carrier. Based on their results, the prepared SN38-carrying chitosan–MUC-1 could be an efficient actively targeted, soluble and low-toxicity anticancer drug for clinical applications.<sup>35</sup> MUC-1 can be used to target only a number of cancer cell lines (pancreatic, epithelial ovarian, invasive lung, prostate, primary lung and breast cancers, and circulating tumor cells).<sup>36</sup> MUC-1, a heavy (80 bp) aptamer, has limitations in targeting and entering the most cancerous cell lines using shape complementarity. However, AS1411 aptamer, a 26 bp single-strand

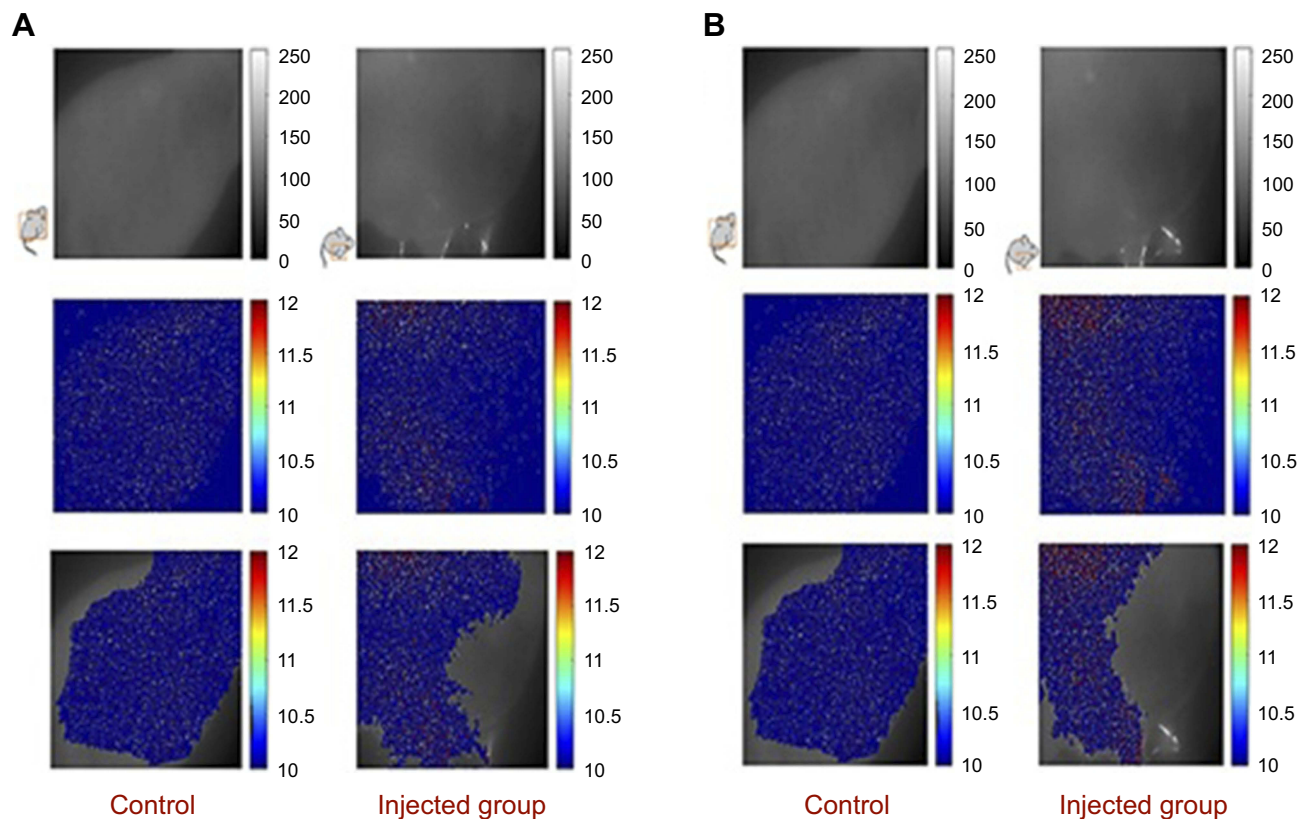


**Figure 12** Accumulation of ASI411–chitosan labeled by BODIPY FL in tumor site: (A) 1 hour and (B) 2 hours after injection.

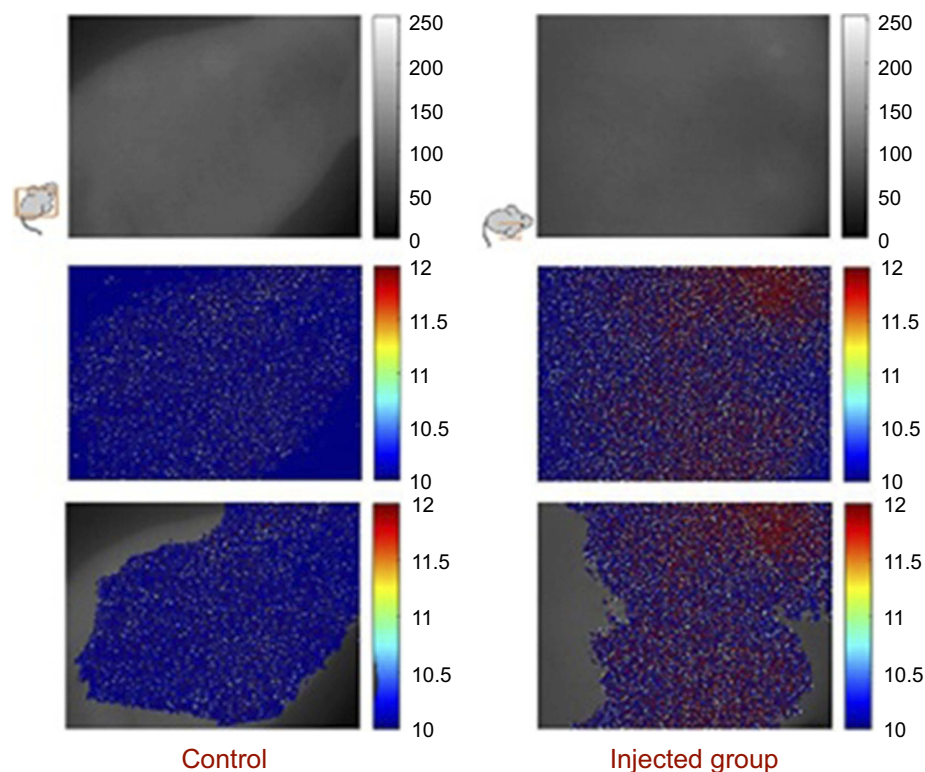


**Figure 13** Accumulation of ASI411–chitosan labeled by BODIPY FL in liver 2 hours after injection.

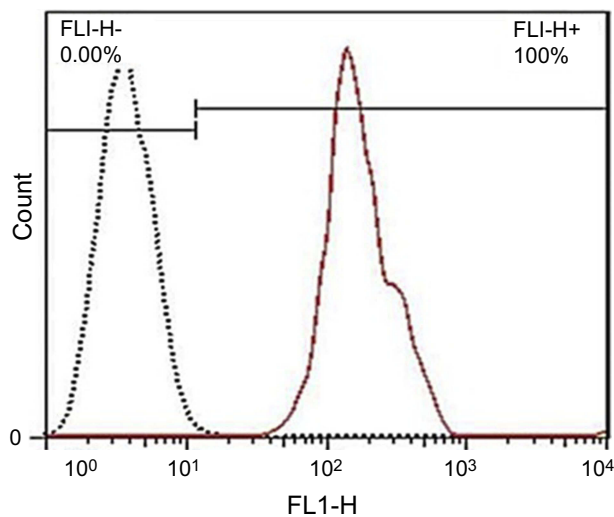


**Figure 14** In vitro cellular uptake of BODIPY FL-labeled ASI411–chitosan conjugates into the T47D cells using flow cytometry. From the graph, uptake is more than 50% (ie, 58%) for the conjugates (red) compared to the untreated control (black).

oligonucleotide, can target a number of different cancer cells. Small aptamers can facilitate uptake of the nanoparticle/drug/agent and their delivery to the tissue or cell of interest.<sup>32,37</sup> According to the results, it can be seen that there was a good uptake of the labeled conjugate to the

T47D cells. In vivo fluorescence imaging showed considerable uptake in the tumor site at 1 and 2 hours after injection. Increased uptake in the liver at 2 hours after injection indicated that the majority of the metabolic processes of labeled ASI411–chitosan probably took place in the liver.

The useful properties of chitosan nanoparticles are not limited to cancer therapy applications; they can also be utilized in diagnostic techniques. As an example, in 2018, Choi et al reported that iodine–echogenic glycol chitosan nanoparticles can be used as efficient CT and ultrasound imaging agents for tumor diagnosis.<sup>38</sup> For decades, delivering imaging or therapeutic agents through the blood–brain barrier has been a serious challenge in diseases such as epilepsy, and the use of nanoparticles helps scientists to overcome this limitation. For instance, Kaur et al reported on an engineered PLGA–chitosan nanoparticle used to transport anti-epileptic TRH analogs targeted to the brain through intranasal delivery.<sup>39</sup>

All in all, data on the in vitro cellular uptake of BODIPY-labeled chitosan–ASI411 aptamer conjugate into T47D cells and their toxicity in cancerous (T47D) and normal (HEK-293) cells showed promising results, which confirmed it as a novel diagnostic agent that can be used in cancer detection

in the future. However, more studies on the in vivo behavior of this conjugate need to be conducted.

## Conclusion

This research investigated the effects of BODIPY-labeled chitosan–AS1411 aptamer conjugates on breast cancer cells (T47D) compared to normal kidney cells (HEK-293). Based on the data yielded, this conjugate can be used as a potential diagnostic agent for fluorescent imaging of cancer cells, with no cellular toxicity on normal cells.

## Acknowledgments

Tehran University of Medical Sciences supported this study. Authors would like to acknowledge all the technicians for their support during the experiments and Tehran University of Medical Sciences Preclinical Core Facility (TPCF), Tehran, Iran, for providing the in vivo imaging and image processing services for this research (for more information visit [www.TPCF.ir](http://www.TPCF.ir)).

## Disclosure

The authors declare no conflicts of interest in this work.

## References

- Islami F, Miller KD, Siegel RL, Fedewa SA, Ward EM, Jemal A. Disparities in liver cancer occurrence in the United States by race/ethnicity and state. *CA Cancer J Clin.* 2017;67(4):273–289. doi:10.3322/caac.21402
- McGuire S. World cancer report 2014. Geneva, Switzerland: World Health Organization, international agency for research on cancer, WHO press, 2015. *Adv Nutr.* 2016;7(2):418–419. doi:10.3945/an.116.012211
- Etemadi A, Sadjadi A, Semnani S, Nouraei M, Khademi H, Bahadori M. *Cancer Registry in Iran: A Brief Overview. Vol. 112008.*
- Mousavi SM, Montazeri A, Mohagheghi MA, et al. Breast cancer in Iran: an epidemiological review. *Breast J.* 2007;13(4):383–391. doi:10.1111/j.1524-4741.2007.00446.x
- Choi KS, Jun JK, Suh M, et al. Effect of endoscopy screening on stage at gastric cancer diagnosis: results of the national cancer screening programme in Korea. *Br J Cancer.* 2015;112(3):608–612. doi:10.1038/bjc.2014.608
- Smith RA, Manassaram-Baptiste D, Brooks D, et al. Cancer screening in the United States, 2015: a review of current American cancer society guidelines and current issues in cancer screening. *CA Cancer J Clin.* 2015;65(1):30–54. doi:10.3322/caac.21261
- Heitzer E, Ulz P, Geigl JB. Circulating tumor DNA as a liquid biopsy for cancer. *Clin Chem.* 2015;61(1):112–123. doi:10.1373/clinchem.2014.222679
- Imperiale TF, Ransohoff DF, Itzkowitz SH, et al. Multitarget stool DNA testing for colorectal-cancer screening. *N Engl J Med.* 2014;370(14):1287–1297. doi:10.1056/NEJMoa1311194
- Li J, Pu K. Development of organic semiconducting materials for deep-tissue optical imaging, phototherapy and photoactivation. *Chem Soc Rev.* 2019;48(1):38–71. doi:10.1039/c8cs00001h
- Watanabe T, Hirano K, Takahashi A, et al. Nucleolin on the cell surface as a new molecular target for gastric cancer treatment. *Biol Pharm Bull.* 2010;33(5):796–803. doi:10.1248/bpb.33.796
- Reyes-Reyes EM, Teng Y, Bates PJ. A new paradigm for aptamer therapeutic AS1411 action: uptake by macropinocytosis and its stimulation by a nucleolin-dependent mechanism. *Cancer Res.* 2010;70(21):8617–8629. doi:10.1158/0008-5472.CAN-10-0920
- Wu J, Song C, Jiang C, Shen X, Qiao Q, Hu Y. Nucleolin targeting AS1411 modified protein nanoparticle for antitumor drugs delivery. *Mol Pharm.* 2013;10(10):3555–3563. doi:10.1021/mp300686g
- Ai J, Xu Y, Lou B, Li D, Wang E. Multifunctional AS1411-functionalized fluorescent gold nanoparticles for targeted cancer cell imaging and efficient photodynamic therapy. *Talanta.* 2014;118:54–60. doi:10.1016/j.talanta.2013.09.062
- Rosenberg JE, Bambury RM, Van Allen EM, et al. A phase II trial of AS1411 (a novel nucleolin-targeted DNA aptamer) in metastatic renal cell carcinoma. *Invest New Drugs.* 2014;32(1):178–187. doi:10.1007/s10637-013-0045-6
- Park S-M, Aalipour A, Vermesh O, Yu JH, Gambhir SS. Towards clinically translatable in vivo nanodiagnosics. *Nat Rev Mater.* 2017;2:17014. 05/03/online. doi:10.1038/natrevmats.2017.14
- Mortazavi Y, Ghoreishi SM. Synthesis of mesoporous silica and modified as a drug delivery system of ibuprofen. *J Nanostruct.* 2016;6(1):86–89.
- Wang EC, Wang AZ. Nanoparticles and their applications in cell and molecular biology. *Integrative Biology.* 2014;6(1):9–26. doi:10.1039/c3ib40165k
- Miao Q, Xie C, Zhen X, et al. Molecular afterglow imaging with bright, biodegradable polymer nanoparticles. *Nat Biotechnol.* 2017;35:1102. 10/16/online.
- Mortazavi-Derazkola S, Naimi-Jamal MR, Ghoreishi SM. Synthesis, characterization, and atenolol delivery application of functionalized mesoporous hydroxyapatite nanoparticles prepared by microwave-assisted co-precipitation method. *Curr Drug Deliv.* 2016;13(7):1123–1129.
- Kamat V, Bodas D, Paknikar K. Chitosan nanoparticles synthesis caught in action using microdroplet reactions. *Sci Rep.* 2016;6:22260. 02/29/online. doi:10.1038/srep22260
- Mohammed MA, Syeda J, Wasan KM, Wasan EK. An overview of chitosan nanoparticles and its application in non-parenteral drug delivery. *Pharmaceutics.* 2017;9(4):53. doi:10.3390/pharmaceutics9040053
- Bilensoy E. Cationic nanoparticles for cancer therapy. *Expert Opin Drug Deliv.* 2010;7(7):795–809. doi:10.1517/17425247.2010.485983
- Jain K, Kesharwani P, Gupta U, Jain NK. Dendrimer toxicity: let's meet the challenge. *Int J Pharm.* 2010;394(1–2):122–142. doi:10.1016/j.ijpharm.2010.04.027
- Imamura T, Saitou T, Kawakami R. In vivo optical imaging of cancer cell function and tumor microenvironment. *Cancer Sci.* 2018;109(4):912–918. doi:10.1111/cas.13544
- Solomon M, Liu Y, Berezin MY, Achilefu S. Optical imaging in cancer research: basic principles, tumor detection, and therapeutic monitoring. *Med principles practice.* 2011;20(5):397–415. doi:10.1159/000327655
- Ghoreishi SM, Khalaj A, Sabzevari O, et al. Technetium-99m chelator-free radiolabeling of specific glutamine tumor imaging nanoprobe: in vitro and in vivo evaluations. *Int J Nanomedicine.* 2018;13:4671–4683. doi:10.2147/IJN.S157426
- Mohammadzadeh P, Cohan RA, Ghoreishi SM, Bitarafan-Rajabi A, Ardestani MS. AS1411 aptamer-anionic linear globular dendrimer G2-Iohexol selective nano-theranostics. *Sci Rep.* 2017;7(1):11832. doi:10.1038/s41598-017-12150-8
- Barzegar Behrooz A, Nabavizadeh F, Adiban J, et al. Smart bomb AS1411 aptamer-functionalized/PAMAM dendrimer nanocarriers for targeted drug delivery in the treatment of gastric cancer. *Clin Exp Pharmacol Physiol.* 2017;44(1):41–51. doi:10.1111/1440-1681.12670

29. Azhdarzadeh M, Atyabi F, Saei AA, et al. Theranostic MUC-1 aptamer targeted gold coated superparamagnetic iron oxide nanoparticles for magnetic resonance imaging and photothermal therapy of colon cancer. *Colloids Surf B*. 2016;143:224–232. doi:10.1016/j.colsurfb.2016.02.058
30. Soundararajan S, Chen W, Spicer EK, Courtenay-Luck N, Fernandes DJ. The nucleolin targeting aptamer AS1411 destabilizes Bcl-2 messenger RNA in human breast cancer cells. *Cancer Res*. 2008;68(7):2358–2365. doi:10.1158/0008-5472.CAN-07-5723
31. Ireson CR, Kelland LR. Discovery and development of anticancer aptamers. *Mol Cancer Ther*. 2006;5(12):2957–2962. doi:10.1158/1535-7163.MCT-06-0172
32. Keefe AD, Pai S, Ellington A. Aptamers as therapeutics. *Nat Rev Drug Discovery*. 2010;9(7):537. doi:10.1038/nrd3141
33. Barbas AS, Mi J, Clary BM, White RR. Aptamer applications for targeted cancer therapy. *Future Oncol*. 2010;6(7):1117–1126. doi:10.2217/fon.10.67
34. Fan X, Guo Y, Wang L, Xiong X, Zhu L, Fang K. Diagnosis of prostate cancer using anti-PSMA aptamer A10-3.2-oriented lipid nanobubbles. *Int J Nanomedicine*. 2016;11:3939–3950. doi:10.2147/IJN.S112951
35. Sayari E, Dinarvand M, Amini M, et al. MUC1 aptamer conjugated to chitosan nanoparticles, an efficient targeted carrier designed for anticancer SN38 delivery. *Int J Pharm*. 2014;473(1–2):304–315. doi:10.1016/j.ijpharm.2014.05.041
36. Nabavinia MS, Gholoobi A, Charbgo F, Nabavinia M, Ramezani M, Abnous K. Anti-MUC1 aptamer: a potential opportunity for cancer treatment. *Med Res Rev*. 2017;37(6):1518–1539. doi:10.1002/med.21462
37. Cerchia L, de Franciscis V. Targeting cancer cells with nucleic acid aptamers. *Trends Biotechnol*. 2010;28(10):517–525. doi:10.1016/j.tibtech.2010.07.005
38. Choi D, Jeon S, You DG, et al. Iodinated echogenic glycol chitosan nanoparticles for X-ray CT/US dual imaging of tumor. *Nanotheranostics*. 2018;2(2):117–127. doi:10.7150/ntno.18643
39. Kaur S, Manhas P, Swami A, et al. Bioengineered PLGA-chitosan nanoparticles for brain targeted intranasal delivery of antiepileptic TRH analogues. *Chem Eng J*. 2018;346:630–639. doi:10.1016/j.cej.2018.03.176

## International Journal of Nanomedicine

Dovepress

### Publish your work in this journal

The International Journal of Nanomedicine is an international, peer-reviewed journal focusing on the application of nanotechnology in diagnostics, therapeutics, and drug delivery systems throughout the biomedical field. This journal is indexed on PubMed Central, MedLine, CAS, SciSearch®, Current Contents®/Clinical Medicine,

Journal Citation Reports/Science Edition, EMBase, Scopus and the Elsevier Bibliographic databases. The manuscript management system is completely online and includes a very quick and fair peer-review system, which is all easy to use. Visit <http://www.dovepress.com/testimonials.php> to read real quotes from published authors.

Submit your manuscript here: <https://www.dovepress.com/international-journal-of-nanomedicine-journal>